Electronic Supplementary Information

Multifunctional Au nanoclusters for targeted bioimaging and enhanced photodynamic inactivation of *Staphylococcus aureus*

Boris Khlebtsov,[a,b] Elena Tuchina,[b] Valery Tuchin,[b,c,d] and Nikolai Khlebtsov[a,b,*]

[a] Institute of Biochemistry and Physiology of Plants and Microorganisms, Russian Academy of Sciences, 13 Prospekt Entuziastov, Saratov 410049, Russia

[b] Chernyshevsky Saratov State University, 83 Ulitsa Astrakhanskaya, Saratov 410012, Russia

[c] Institute of Precise Mechanics and Control, Russian Academy of Sciences, 24 Ulitsa Rabochaya, Saratov 410028, Russia

[d] Tomsk State University, 36 Prospekt Lenina, Tomsk 634050, Russia

*E-mail: khlebtsov@ibppm.sgu.ru

S1. Synthesis of Au–HSA NCs and additional characterization of Au–BSA and Au–BSA-PS NCs

For synthesis of Au–HAS NCs, 5 mL of 4.8 mM $HAuCl_4$ was added to 5 mL of an HSA solution (20 mg/mL) under vigorous magnetic stirring for 2 min. Then, 200 mL of 1M NaOH was added. This mixture was heated in an oil bath at 100 ºC for 30 min under vigorous magnetic stirring. After the solution had been cooled to room temperature, the product was collected with an Amicon Ultra-15 centrifuge concentrator (MW cutoff, 10000) and was redispersed in 10 mL of 10 mM PBS (pH 7.4). The final HSA concentration was 10 mg/mL.

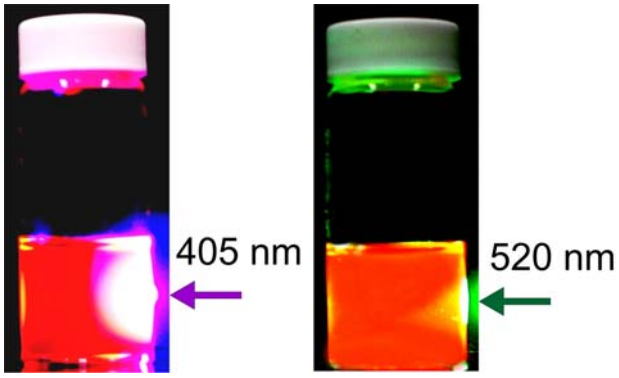

Figure S1. Photos of Au–BSA solutions under side illumination by 450-nm (left) and 520-nm (right) LEDs.

Here, we present simple calculations to evaluate the structural relations for Au–BSA and Au–BSA–PS NCs. According to our synthesis protocol, the number of Au atoms (5 mL of 11.6 mM $HAuCl_4$) in 1 mL of the final solution (19 mL) can be estimated as follows: $N_{Au} = (5\times10^{-3})\times(11.6\times10^{-3})\times6\times10^{23}/19 = 1.83\times10^{18}$. Similarly, the number of BSA molecules in 1 mL of the final solution at a BSA concentration of 10 mg/mL equals $N_{BSA} = (10\times10^{-3})\times(6\times10^{23}/66500) = 0.9\times10^{17}$ molecules of BSA. Here, the molar mass of BSA 66500 was used. Finally, for the ratio N_{Au}/N_{BSA} we get $N_{Au}/N_{BSA} = 1.83\times10^{18}/0.9\times10^{17} = 20$. This value is in reasonable agreement with the reported ratios of 20 and 25 [S1, S2].

Consider now the average number of PS molecules per one Au–BSA–PS complex. The PS loading content was evaluated by measuring the absorption at 675 nm with a molar extinction coefficient of 0.5 $M^{-1}cm^{-1}$ (as determined from the calibration plot, Section S5 below) after subtracting the absorbance of Au–BSA NCs at 675 nm. Typically, the ratio between the BSA and PS concentrations in the final solution equals (2 mg/L)/(2 μg/mL). Taking into account the molar masses of BSA (66500 g/mol) and PS (254 g/mol), we get $N_{PS}/N_{BSA} = 0.26$. Assuming each Au–BSA–PS complex to be bound with only one BSA molecule, we conclude that 10 complexes contain about 3 PS molecules. Despite such a low PS load, the final solutions demonstrate very distinct PS absorption peaks. Clearly, a higher PS load would result in dominant PS absorption and in the optical features of the Au–BSA complexes becoming indistinguishable on the PS background. It is instructive to compare our loading data with those reported by Cui and coworkers [S3] for GSH-capped Au–GSH complexes containing NHS-activated FA-conjugated PEG (FA–PEG_{2K}–NHS) and loaded with the Ce6 drug. In contrast to our protocol with a very low PS:BSA~PS:NC weight ratio (1:100), those authors used a much higher Ce6:NC weight ratio (1:4). The Ce6 weight load was determined to be 0.06 (6%), much higher than our PS weight load of about 0.001 (0.1%). Unfortunately, there is no information about the precise molecular formula of the NCs synthesized in Ref. [S3]. For approximate estimations, we assume the NC formula to be $Au_{22}(SG)_{18,}$ as found by Xei and coworkers [S4] for highly fluorescent GSH NCs with a QY of 8%, in agreement with the QY value measured in Ref. [S3]. Taking into account the molar mass $[GSH]_{18}$ = 5526, [FA] = 441, [Ce6] = 840, [PEG2k] = 2000, and $[Au_{18}]$ = 3546, we get a molar mass of the Au–GSH–PEG2k–FA–Ce6 complexes of 12353. Accordingly, the number of Ce6 per NC complex is 12353×0.06/840 = 0.88. This means that 10 Au–GSH–PEG2k–

FA–Ce6 complexes contain about 9 Ce6 molecules. Thus, despite the difference in the average weight load being almost two orders of magnitude, the number of Ce6 per complex is greater than our estimate (~3) by three times only.

S2. Evaluation of the Au–BSA NC size

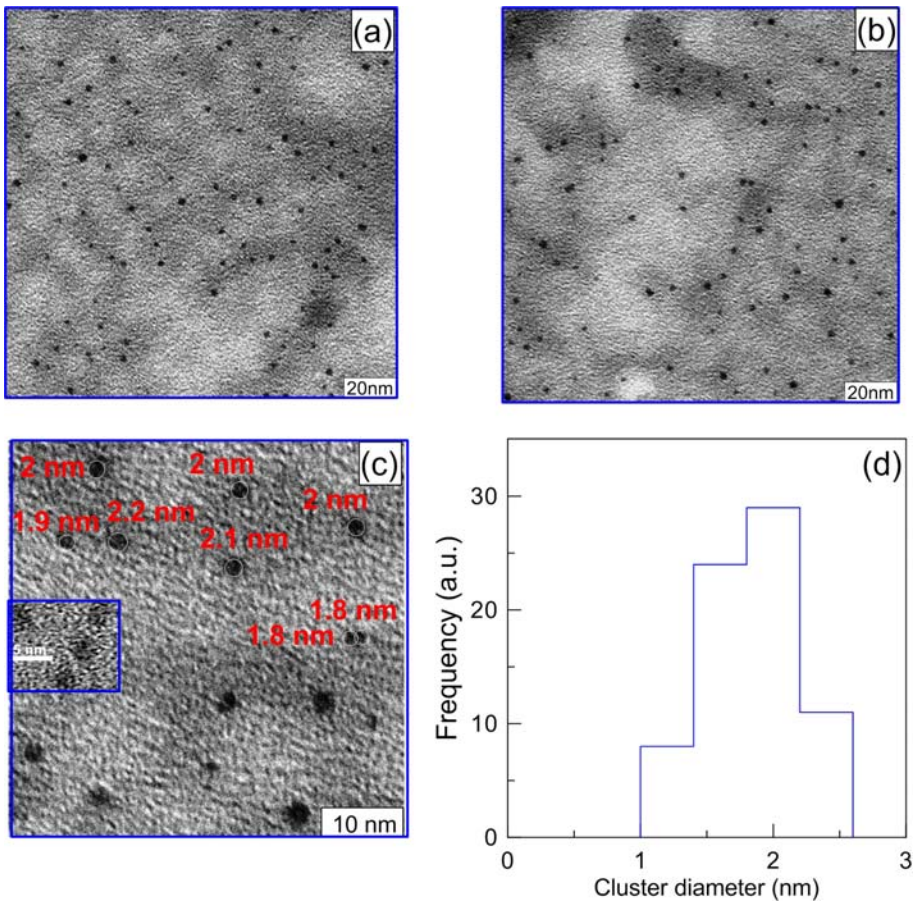

Figure S2. Representative TEM images of Au–BSA NCs (a, b, c) and the size-distribution histogram derived from 100 NCs (c). The average NC diameter is 1.8 ± 0.4 nm. The inset in panel (c) shows an HRTEM image of clusters with an average size of 1.12 ± 0.43 nm, as estimated by Sahoo et al. (*ACS Appl. Mater. Interfaces*, 2014, **6**, 712). The scale bars [5 nm in the inset and 10 nm in panel (c)] were adjusted for equal magnification. Note that the NCs in the inset look similarly to those in panel (c) despite the difference in the average size estimation.

Table 1S. TEM-sizes of Au-BSA and some related NCs

Cluster type	Size (nm)	Reference
Au_{25}–BSA (MALDI–TOF)	1 (TEM)	[S5] Xie 2009
Au_{25}–BSA (MALDI–TOF)	1 (TEM)*	[S6] Dong 2015
Au–BSA	2 (TEM)	[S7] Wang 2011
Au–BSA	2.4 (TEM)	[S8] Zhou 2013
Au_{25}–BSA (MALDI–TOF)	2.5 (DLS)	[S9] Das 2012
Au_{20}–BSA (MALDI–TOF)	2.6 (TEM, HRTEM)	[S10] Zhang 2014
Au–BSA	~3 (TEM)	[S11] Lin 2013
Au–BSA	5 (HRTEM)	[S12] Ding 2015
Au–GSH, Au–BSA	2 (TEM), 8 (TEM)	[S13] Zhang 2912
Au–BSA	1–8 (TEM)	[S14] Retnakumari 2010
Au_{25}–SG_{18} (ESI–MS)[$]	1 (TEM) QY<1%	[S15] Wu 2011
Au_{25}–SG_{18}	1.4 (TEM)	[S16] Niesen 2014
Au_{20}–MPA_{15} (MALDI–TOF)[#]	0.6–2.2 (TEM, HRTEM) Dav=1.1 nm	[S17] Sahoo 2014
Au–GSH	2 (TEM, HRTEM)	[S3] Zhang 2015

* From the TEM images, the average size seems to be about 2 nm

[$] ESI–MS – Electrospray ionization mass spectrometry

[#]MPA – Mercaptopropionic acid; MALDI–TOF – Matrix-assisted laser desorption/ionization time-of-flight (MALDI–TOF) mass spectrometry

S3. Measuring the QY of the Au–BSA NCs

For evaluating the QY of the Au–BSA NCs, a hematoporphyrin (HP) solution in PBS was chosen as a benchmark standard, as the red emission spectrum of HP is located within the red emission band of Au–BSA NCs and the QY value of HP is known from the literature [S18, S19]. Only diluted solutions with an absorbance of 0.05 at the excitation wavelength were used in order to exclude the "inner-filter effect" [S20, S21]. Under these conditions, the QY can be calculated by Eq. (2) of the manuscript. According to Figure S2, the ratio between the areas under the sample and reference emission spectra is 10123/19297. Thus, after multiplying by the reference QY_r = 25%, we get QY = (10123/18297)×25% = 13.8%.

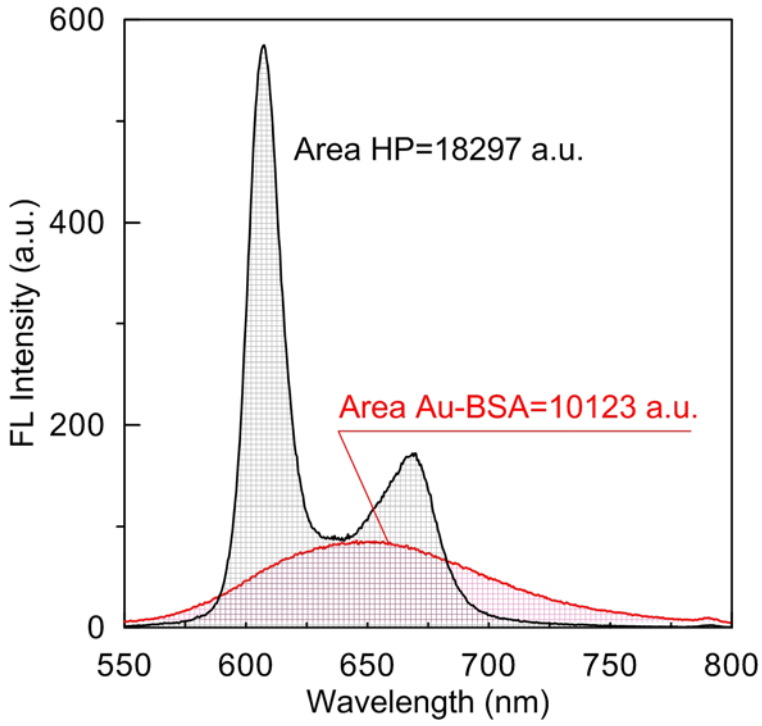

Figure S3. Emission spectra of hematoporphyrin (HP) and Au–BSA NCs in PBS under 405-nm excitation.

S4. Dot immunoassay of Au–BSA–IgG NCs

Colloidal gold nanoparticles (CG NPs) were prepared by the reduction of tetrachloroauric acid with sodium citrate [S22, S23]. The mean particle diameter (15 nm) and the number concentration (1.4×10^{12} particles/ml) were determined by spectrophotometric calibrations [S23, S24, 25]. Ten μg of Au–BSA–IgG (10 μL of an aqueous 1-mg/mL solution) was added to 1 mL of the initial suspension of Au NPs (or 15-nm CG) so as to achieve stabilization against aggregation caused by adding NaCl to a final concentration of 1%. The conjugates of

the Au NPs were centrifuged and redispersed in a PBS containing 0.04% PEG, to ensure their secondary stabilization.

The dot assay was done on a nitrocellulose membrane (Schleicher & Schuell, Germany). In a typical protocol [S26], 1 μL of a protein A solution or 3 μL of an MRSA suspension were spotted onto the membrane in the center of a drawn 5-mm square. Then, 12 analyte samples were obtained by sequential double dilutions of the initial solutions (1 mg/mL) and were analyzed in one test. After 30 min of absorption, the membrane was incubated in a blocking buffer of 0.1 % PEG (MW, 20,000; Sigma, USA), 150 mM NaCl, and 20 mM Tris–HCl (pH 8.2) at room temperature for 30 min. Next, the membrane with applied analytes was placed in a suspension of Au–BSA–IgG–CG or Au–BSA–IgG conjugates for 30 min. With the Au–BSA–IgG-CG complexes, the biospecific binding could be observed as red spots under white light illumination owing to the plasmonic absorption of CG near 520 nm (Fig. S4 a). In the second case, we observed red FL of Au–BSA NCs under UV illumination (Fig. S4 b). Finally, no biospecific binding was seen for the negative controls with nontargeted probes CG_{15nm} + Au–BSA (Fig. S4 c) and Au–BSA (Fig. S4 d).

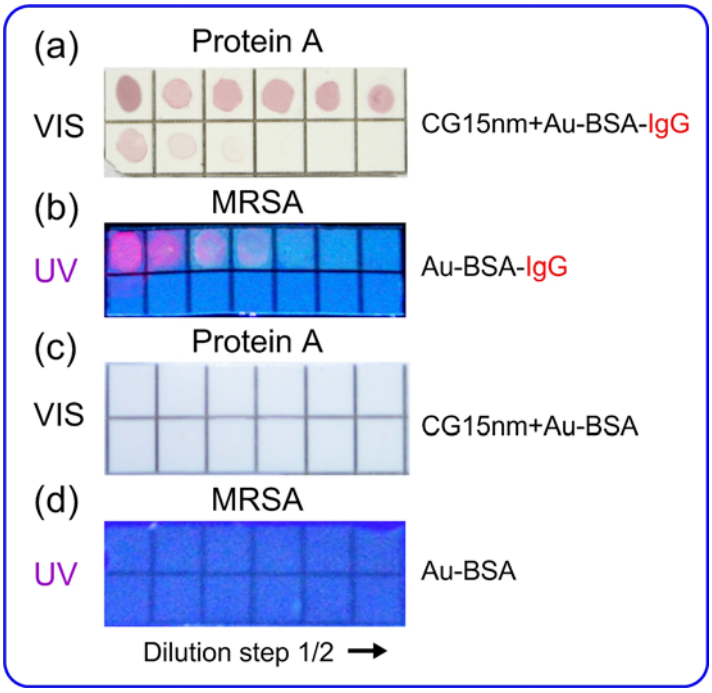

Figure S4. Dot assay of protein A (3 μL; concentration, 1 mg/mL; sequential double dilutions) by using CG_{15nm} + Au–BSA–IgG conjugates and white light illumination (a) and dot assay of MRSA (3 μL; absorbance, 0.9 at 600 nm; sequential double dilutions) by using Au–BSA–IgG NCs and UV illumination (b). The panels (c) and (d) show controls with nontargeted probes (CG_{15nm} + Au–BSA and Au–BSA, respectively). The blue color of the panels (b) and (d) under UV irradiation is due to autofluorescence.

S5. Calibration plot for determination of the PS concentration

Figure S5a shows the extinction spectra of PS solutions with concentrations ranging from 0.25 μg/mL to 32 μg/mL . The calibration plot (Fig. S2b) was obtained at an absorption maximum wavelength of 675 nm. The extinction coefficient was estimated to be 0.2 $(\mu g/mL)^{-1}$ cm^{-1}. Taking into account the PS molar mass of 254 g/mol, we get a molar extinction coefficient of 0.5 M^{-1} cm^{-1}.

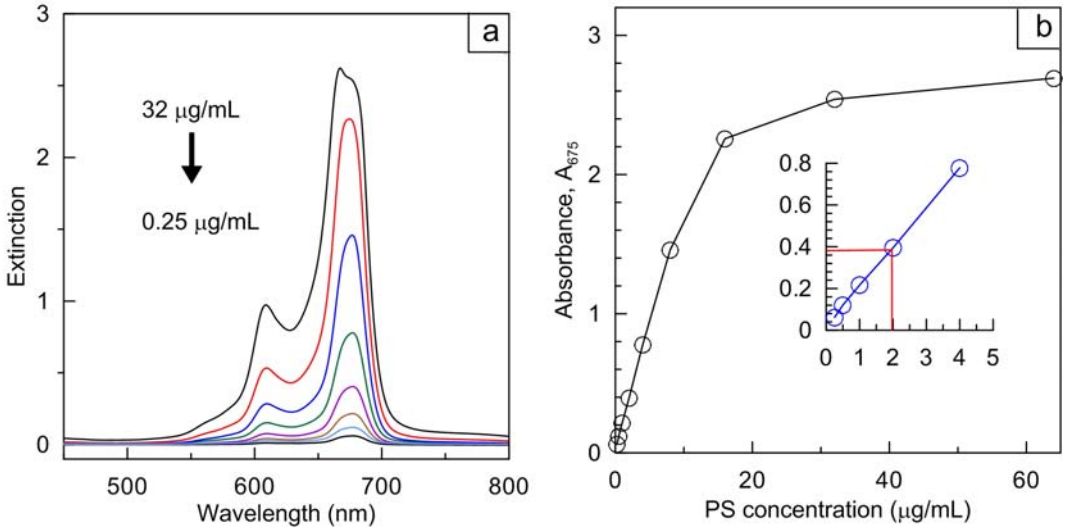

Figure S5. (a) Extinction spectra of Photosens (PS) solutions in PBS with concentrations ranging from 32 to 0.25 μg/mL (double dilutions). (b) Calibration plot for determination of the PS concentration from the absorbance at 675 nm. The inset illustrates the determination of the PS concentration for a solution of Au–BSA–PS complexes.

S6. Absorbance spectra of PS, NCs, and the complexes in the spectral band 230-400 nm

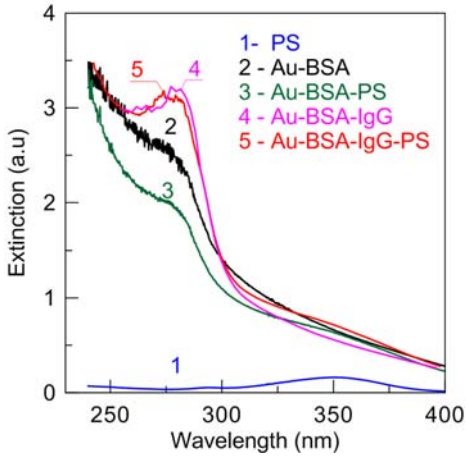

Figure S6. Short-wavelength (230–400 nm) extinction spectra of a PS solution (2 μg/mL) in PBS (1), Au–BSA NCs (2), and the complexes Au–BSA–PS (3), Au–BSA–IgG (4), and Au–

BSA–IgG–PS (5). The UV shoulders of spectra (2) and (3) are due to BSA absorption, and the UV peaks of spectra (4) and (5) in UV are due to IgG absorption.

S7. Binding of Au–BSA and Au–HSA NCs to bacteria at pH 4 and 6

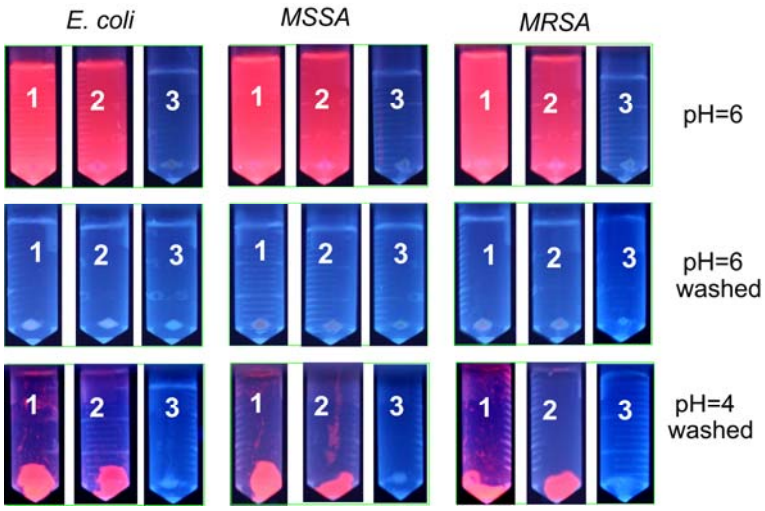

Figure S7. Photos under UV illumination obtained after incubation of *E. coli*, MSSA, and MRSA with Au–BSA (1), Au–HSA (2), and PBS (3). All samples are under UV illumination. The red color corresponds to NC FL. The top row was obtained at pH 6, and the middle and bottom rows were obtained after centrifugation and washing (pH 6 and 4, respectively). No FL is observed for the negative control (*E. coli*) and for MSSA and MRSA in PBS, weak red FL is observed for samples (1) and (2) at pH 6, and intense FL is seen for samples 1 and 2 with MSSA and MRSA at pH 4. Clearly, the aggregation of MSSA and MRSA is caused by the nonspecific adsorption of the Au–BSA and Au–HSA complexes at pH below the isoelectric point.

References

S1 P. Zhang, X. X. Yang, Y. Wang, N. W. Zhao, Z. H. Xiong and C. Z. Huang, *Nanoscale*, 2014, **6**, 2261.

S2 X. Wen, P. Yu, Y.-R. Toh and J. Tang, *J. Phys. Chem. C*, 2012, **116**, 11830.

S3 C. Zhang, C. Li, Y. Liu, J. Zhang, C. Bao, S. Liang, Q. Wang, Y. Yang, H. Fu, K. Wang and D. Cui, *Adv. Func. Mater.*, 2015, **25**, 1314.

S4 Y. Yu, Z. Luo, D. M. Chevrier, D. T. Leong, P. Zhang, D. Jiang and J. Xie, *J. Am. Chem. Soc.*, 2014, **136**, 1246.

S5 J. Xie, Y. Zheng and J. Y. Ying, *J. Am. Chem. Soc.*, 2009, **131**, 888.

S6 L. Dong, M. Li, S. Zhang, J. Li, G. Shen, Y. Tu, J. Zhu and J. Tao, *Small*, 2015, **11**, 2571.

S7 Y. Wang, J. Chen and J. Irudayaraj, *ACS Nano*, 2011, **5**, 9718.

S8 Z. Zhou, C. Zhang, Q. Qian, J. Ma, P. Huang, X. Zhang, L. Pan, G. Gao, H. Fu, S. Fu, H. Song, X. Zhi, J. Ni and D. Cui, *J. Nanobiotechnology*, 2013, **11**, 17.

S9 T. Das, P. Ghosh, M. S. Shanavas, A. Maity, S. Mondal and P. Purkayastha, *Nanoscale*, 2012, **4**, 6018.

S10 P. Zhang, X. X. Yang, Y. Wang, N. W. Zhao, Z. H. Xiong and C. Z. Huang, *Nanoscale*, 2014, **6**, 2261.

S11 J. Lin, Z. Zhou, Z. Li, C. Zhang, X. Wang, K. Wang, G. Gao, P. Huang and D. Cui, *Nanoscale Res. Lett.*, 2013, **8**, 170.

S12 C. Ding and Y. Tian, *Biosensors and Bioelectronics*, 2015, **65**,183.

S13 X.-D. Zhang, D. Wu, X. Shen, P.-X. Liu, F.-Y. Fan and S.-J. Fan, *Biomaterials*, 2012, **33**, 4628.

S14 A. Retnakumari, S. Setua, D. Menon, P. Ravindran, H. Muhammed, T. Pradeep, S. Nair and M. Koyakutty, *Nanotechnology*, 2010, **21,** 055103.

S15 Z. Wu, J. Chen and R. Jin, *Adv. Funct. Mater.*, 2011, **21**, 177.

S16 B. Niesen and B. P. Rand, *Adv. Mater*., 2014, **26**, 1446.

S 17 A. K. Sahoo, S. Banerjee, S. S. Ghosh and A. Chattopadhyay, *ACS Appl. Mater. Interfaces*, 2014, **6**, 712.

S 18 A. Andreoni, R. Cubeddu, S. De Silvestri, G. Jori, P. Laporta and E. Reddi, *Z. Naturforsch.*, 1983, **38**, 83.

S19 G. Cauzzo, C. Gennari, G. Jori and J. D. Spikes, *Photochem. Photobiol*. 1977, **25**, 389.

S20 J. R. Lakowicz, *Principles of Fluorescence Spectroscopy*. 3-rd ed., Springer, New York 2006.

S21 D. F. Eaton, *J. Photochem. Photobiol. B*, 1988, **2**, 523.

S22 G. Frens, *Nature Phys. Sci*., 1973, **241**, 20.

S23 N. G. Khlebtsov, V. A. Bogatyrev, L. A. Dykman and A. G. Melnikov, *J. Colloid Interface Sci*., 1996, **180**, 436.

S24 W. Haiss, N. T. K. Thanh, J. Aveard and D. G. Fernig, *Anal. Chem*., 2007, **79**, 4215.

S25 N. G. Khlebtsov, *Anal. Chem*., 2008, **80**, 6620.

S26 B. N. Khlebtsov and N. G. Khlebtsov, *Nanotechnology*, 2008, **19**, 435703.